ICSV14

Cairns • Australia

9-12 July, 2007

14th International Congress on Sound & Vibration

WEIGHTED STATISTICALLY OPTIMISED NEAR FIELD ACOUSTIC HOLOGRAPHY WITH PRESSURE-VELOCITY PROBES

Finn Jacobsen[1], Xinyi Chen[1] and Virginie Jaud[2]

[1]Acoustic Technology, Ørsted•DTU, Technical University of Denmark, Building 352, DK-2800 Kgs. Lyngby, Denmark

[2]Extraction et Exploitation de l'Information en Environnements Incertains, École Nationale Supérieure d'Ingénieurs des Études des Techniques d'Armement, 2 rue François Verny, F-29806 Brest Cedex 9, France

fja@oersted.dtu.dk

Abstract

Statistically optimised near field acoustic holography (SONAH) differs from conventional near field acoustic holography (NAH) by avoiding discrete spatial Fourier transforms. Both NAH and SONAH are based on the assumption that all sources are on one side of the measurement plane whereas the other side is source free. An extension of the SONAH procedure based on measurement with an array of pressure-velocity probes has recently been suggested. The pressure-velocity method makes it possible—within limits—to distinguish between sources on the two sides of the array and thus suppress the influence of extraneous noise coming from the 'wrong' side. This paper examines the possibility of improving the performance of the method by modifying some of the parameters used in determining the SONAH transfer matrix.

1. INTRODUCTION

Near field acoustic holography (NAH) is a technique that makes it possible to reconstruct the sound field near a source from measurements on a surface [1]. Statistically optimised near field acoustic holography (SONAH) is an interesting variant of NAH developed a few years ago by Steiner and Hald [2]. SONAH has the advantage of avoiding the discrete spatial Fourier transforms used in NAH and thus the resulting truncation effects [1]; therefore the measurement array can be smaller than the source [2, 3].

NAH and SONAH are usually based on measurement of the sound pressure. However, an acoustic particle velocity transducer has been available for some years [4], and it has recently been demonstrated that NAH and SONAH based on measurement of both the pressure and the normal component of the particle velocity in general give more accurate sound field reconstructions than pressure-based SONAH [5, 6]. An additional advantage of the pressure-velocity technique is that it makes it possible to combine pressure- and velocity-based predictions and thereby be able to distinguish between sound coming from the two sides of the measurement plane in the same way as one can do that with a double layer array of pressure transducers [7, 8]. However, if the level of the disturbing noise is high the pressure-velocity method breaks down

[6]. The purpose of this paper is to examine whether it is possible to improve the performance of pressure- and velocity-based SONAH by modifying some SONAH parameters.

2. A BRIEF OUTLINE OF SONAH THEORY

The SONAH theory has been described eg in refs. [2, 3]; therefore the description given in what follows is very brief and concentrates on factors of particular relevance for this investigation.

2.1 SONAH based on measurement of sound pressure

The SONAH procedure expresses the sound pressure at N positions in the prediction plane as a weighted sum of sound pressures measured at N positions in the hologram plane,

$$\mathbf{p}^{\mathrm{T}}(\mathbf{r}) = \mathbf{p}^{\mathrm{T}}(\mathbf{r}_h)\mathbf{c}(\mathbf{r}) = \mathbf{p}^{\mathrm{T}}(\mathbf{r}_h)\left(\mathbf{A}^{\mathrm{H}}\mathbf{A} + \theta^2\mathbf{I}\right)^{-1}\mathbf{A}^{\mathrm{H}}\boldsymbol{\alpha}(\mathbf{r}), \tag{1}$$

where $\mathbf{p}^{\mathrm{T}}(\mathbf{r})$ is a transposed column vector with the N pressures in the prediction plane, $\mathbf{p}^{\mathrm{T}}(\mathbf{r}_h)$ is a similar vector with the measured data, $\mathbf{c}(\mathbf{r})$ is the transfer matrix, $\mathbf{A}^{\mathrm{H}}\mathbf{A}$ is a matrix that depends on the N positions in the measurement plane, $\mathbf{A}^{\mathrm{H}}\boldsymbol{\alpha}$ is a matrix that depends on the N positions in the prediction plane and N positions in the measurement plane, $\mathbf{I}$ is the identity matrix, and θ is a regularisation parameter [3]. All matrices are N by N. The transfer matrix $\mathbf{c}(\mathbf{r})$ represents the (regularised) optimal least-squares solution to the overdetermined problem posed by requiring that M propagating and evanescent elementary waves ($M > N$), all having a pressure amplitude of unity in the source plane, satisfy eq. (1). In the limit of $M \to \infty$ the matrices $\mathbf{A}^{\mathrm{H}}\mathbf{A}$ and $\mathbf{A}^{\mathrm{H}}\boldsymbol{\alpha}$ become integrals that can be evaluated numerically [3].

The normal component of the particle velocity in the prediction plane is obtained from the gradient of the pressure using Euler's equation of motion,

$$\mathbf{u}_z^{\mathrm{T}}(\mathbf{r}) = \frac{-1}{\mathrm{j}\omega\rho}\mathbf{p}^{\mathrm{T}}(\mathbf{r}_h)\left(\mathbf{A}^{\mathrm{H}}\mathbf{A} + \theta^2\mathbf{I}\right)^{-1}\frac{\partial\mathbf{A}^{\mathrm{H}}\boldsymbol{\alpha}(\mathbf{r})}{\partial z} = \mathbf{p}^{\mathrm{T}}(\mathbf{r}_h)\left(\mathbf{A}^{\mathrm{H}}\mathbf{A} + \theta^2\mathbf{I}\right)^{-1}\mathbf{A}^{\mathrm{H}}\boldsymbol{\alpha}_u(\mathbf{r}), \tag{2}$$

where the only quantity that is differentiated is the matrix $\mathbf{A}^{\mathrm{H}}\boldsymbol{\alpha}$ since this is the only quantity that depends on z. The matrix $\mathbf{A}^{\mathrm{H}}\boldsymbol{\alpha}_u$ can be expressed in terms of an integral that can be evaluated numerically [3].

2.2 SONAH based on measurement of particle velocity

The normal component of the particle velocity in the prediction plane can also be determined from the normal component of the particle velocity in the measurement plane using the same transfer matrix as in eq. (1),

$$\mathbf{u}_z^{\mathrm{T}}(\mathbf{r}) = \mathbf{u}_z^{\mathrm{T}}(\mathbf{r}_h)\left(\mathbf{A}^{\mathrm{H}}\mathbf{A} + \theta^2\mathbf{I}\right)^{-1}\mathbf{A}^{\mathrm{H}}\boldsymbol{\alpha}(\mathbf{r}), \tag{3}$$

and the corresponding pressure can be determined from an integral of the particle velocity,

$$\mathbf{p}^{\mathrm{T}}(\mathbf{r}) = \mathbf{u}_z^{\mathrm{T}}(\mathbf{r}_h)\left(\mathbf{A}^{\mathrm{H}}\mathbf{A} + \theta^2\mathbf{I}\right)^{-1}(-\mathrm{j}\omega\rho)\int\mathbf{A}^{\mathrm{H}}\boldsymbol{\alpha}(\mathbf{r})\mathrm{d}z = \mathbf{u}_z^{\mathrm{T}}(\mathbf{r}_h)\left(\mathbf{A}^{\mathrm{H}}\mathbf{A} + \theta^2\mathbf{I}\right)^{-1}\mathbf{A}^{\mathrm{H}}\boldsymbol{\alpha}_p(\mathbf{r}), \tag{4}$$

where the only quantity that is integrated is $\mathbf{A}^{\mathrm{H}}\boldsymbol{\alpha}$ since this is the only quantity that depends on z. In the limit of $M \to \infty$ $\mathbf{A}^{\mathrm{H}}\boldsymbol{\alpha}_p$ becomes an integral that can be evaluated numerically [6]. Equations (3) and (4) were derived and examined in ref. [6]. However, inspection leads to the conclusion that they are based on propagating and evanescent elementary waves with a *particle velocity* amplitude of unity in the source plane, unlike eqs. (1) and (2). This might be less than optimal, in particular when pressure- and particle velocity-based estimates are combined.

2.3 Weighted SONAH

With a transfer matrix based on propagating and evanescent elementary waves with a *pressure* amplitude of unity in the source plane eqs. (3) and (4) become

$$\mathbf{u}_z^{\mathrm{T}}(\mathbf{r}) = \mathbf{u}_z^{\mathrm{T}}(\mathbf{r}_h)\left(\mathbf{B}^{\mathrm{H}}\mathbf{B} + \theta^2\mathbf{I}\right)^{-1}\mathbf{B}^{\mathrm{H}}\boldsymbol{\beta}(\mathbf{r}), \tag{5}$$

$$\mathbf{p}^{\mathrm{T}}(\mathbf{r}) = \mathbf{u}_z^{\mathrm{T}}(\mathbf{r}_h)\left(\mathbf{B}^{\mathrm{H}}\mathbf{B} + \theta^2\mathbf{I}\right)^{-1}(-\mathrm{j}\omega\rho)\int \mathbf{B}^{\mathrm{H}}\boldsymbol{\beta}(\mathbf{r})\mathrm{d}z = \mathbf{u}_z^{\mathrm{T}}(\mathbf{r}_h)\left(\mathbf{B}^{\mathrm{H}}\mathbf{B} + \theta^2\mathbf{I}\right)^{-1}\mathbf{B}^{\mathrm{H}}\boldsymbol{\beta}_p(\mathbf{r}), \tag{6}$$

where $\mathbf{B}^{\mathrm{H}}\mathbf{B}$, $\mathbf{B}^{\mathrm{H}}\boldsymbol{\beta}$, and $\mathbf{B}^{\mathrm{H}}\boldsymbol{\beta}_p$ can be expressed in terms of integrals that can be evaluated numerically. Yet another possibility is to modify eqs. (1) and (2) by introducing a transfer matrix based on propagating and evanescent elementary waves with a *particle velocity* amplitude of unity in the source plane,

$$\mathbf{p}^{\mathrm{T}}(\mathbf{r}) = \mathbf{p}^{\mathrm{T}}(\mathbf{r}_h)\left(\mathbf{G}^{\mathrm{H}}\mathbf{G} + \theta^2\mathbf{I}\right)^{-1}\mathbf{G}^{\mathrm{H}}\boldsymbol{\gamma}(\mathbf{r}), \tag{7}$$

$$\mathbf{u}_z^{\mathrm{T}}(\mathbf{r}) = \frac{-1}{\mathrm{j}\omega\rho}\mathbf{p}^{\mathrm{T}}(\mathbf{r}_h)\left(\mathbf{G}^{\mathrm{H}}\mathbf{G} + \theta^2\mathbf{I}\right)^{-1}\frac{\partial \mathbf{G}^{\mathrm{H}}\boldsymbol{\gamma}(\mathbf{r})}{\partial z} = \mathbf{p}^{\mathrm{T}}(\mathbf{r}_h)\left(\mathbf{G}^{\mathrm{H}}\mathbf{G} + \theta^2\mathbf{I}\right)^{-1}\mathbf{G}^{\mathrm{H}}\boldsymbol{\gamma}_u(\mathbf{r}), \tag{8}$$

where $\mathbf{G}^{\mathrm{H}}\mathbf{G}$, $\mathbf{G}^{\mathrm{H}}\boldsymbol{\gamma}$ and $\mathbf{G}^{\mathrm{H}}\boldsymbol{\gamma}_u$ can be expressed in terms of integrals that can be evaluated numerically. All in all there are two pressure-based estimates of the pressure with different weighting of the elementary waves, eqs. (1) and (7); two particle velocity-based estimates of the pressure with different weighting of the elementary waves, eqs. (4) and (6); two pressure-based estimates of the particle velocity with different weighting of the elementary waves, eqs. (2) and (8); and two particle velocity-based estimates of the particle velocity with different weighting of the elementary waves, eqs. (3) and (5).

2.4 SONAH based on measurement of pressure and particle velocity

The fact that particle velocity is a vector component makes it possible to separate the contributions from the 'right' side of the measurement array from contributions from the 'wrong' side [6]. Thus the sound pressure and the particle velocity in 'the primary prediction plane' generated by the source on the 'right' side of the measurement plane can be estimated as the average of a pressure- and a particle velocity-based estimate, and the sound pressure and the particle velocity in 'the secondary prediction plane' generated by the source on the 'wrong' side of the measurement plane can be estimated as half the difference between a pressure- and a particle velocity-based estimate. In what follows this method of combining two estimates based on pressure and particle velocity measurements is referred to as 'the *p-u* method'.

$$\mathbf{p}^{\mathrm{T}}(\mathbf{r}) = ½\left(\mathbf{p}^{\mathrm{T}}(\mathbf{r}_h)\left(\mathbf{A}^{\mathrm{H}}\mathbf{A} + \theta^2\mathbf{I}\right)^{-1}\mathbf{A}^{\mathrm{H}}\boldsymbol{\alpha}(\mathbf{r}) \pm \mathbf{u}_z^{\mathrm{T}}(\mathbf{r}_h)\left(\mathbf{A}^{\mathrm{H}}\mathbf{A} + \theta^2\mathbf{I}\right)^{-1}\mathbf{A}^{\mathrm{H}}\boldsymbol{\alpha}_p(\mathbf{r})\right), \tag{9}$$

$$\mathbf{u}_z^{\mathrm{T}}(\mathbf{r}) = ½\left(\mathbf{p}^{\mathrm{T}}(\mathbf{r}_h)\left(\mathbf{A}^{\mathrm{H}}\mathbf{A} + \theta^2\mathbf{I}\right)^{-1}\mathbf{A}^{\mathrm{H}}\boldsymbol{\alpha}_u(\mathbf{r}) \pm \mathbf{u}_z^{\mathrm{T}}(\mathbf{r}_h)\left(\mathbf{A}^{\mathrm{H}}\mathbf{A} + \theta^2\mathbf{I}\right)^{-1}\mathbf{A}^{\mathrm{H}}\boldsymbol{\alpha}(\mathbf{r})\right). \tag{10}$$

It is worth emphasising that the prediction plane for estimates based on subtracting pressure- and particle velocity-based predictions, here referred to as 'the secondary prediction plane', is the *image plane* of the prediction plane for estimates based on averaging pressure- and particle velocity-based predictions, here referred to as 'the primary prediction plane', since the SONAH system has no way of knowing from which side the sound is coming.

In ref. [6] eqs. (1) and (4) were combined to give the sound pressure, and eqs. (2) and (3) were combined to give the particle velocity. In this investigation variants of the *p-u* method based on the more 'natural' combinations given by eqs. (1) and (6), eqs. (4) and (7), eqs. (2) and (5), and eqs. (3) and (8) are examined.

3. A SIMULATION STUDY

The methods described in the foregoing have been examined in a simulation study. In all test cases there were 8 x 8 pressure and particle velocity transducers in the measurement array; the measurement and prediction plane(s) had dimensions 21 x 21 cm; and the distance between the measurement and prediction plane(s) was 3 cm. The distance between the measurement plane and the plane from which the elementary waves originate, *d*, was 6 cm unless otherwise mentioned. Regularisation was done as in ref. [6] using the generalised cross validation method [9].

3.1 SONAH without a disturbing source

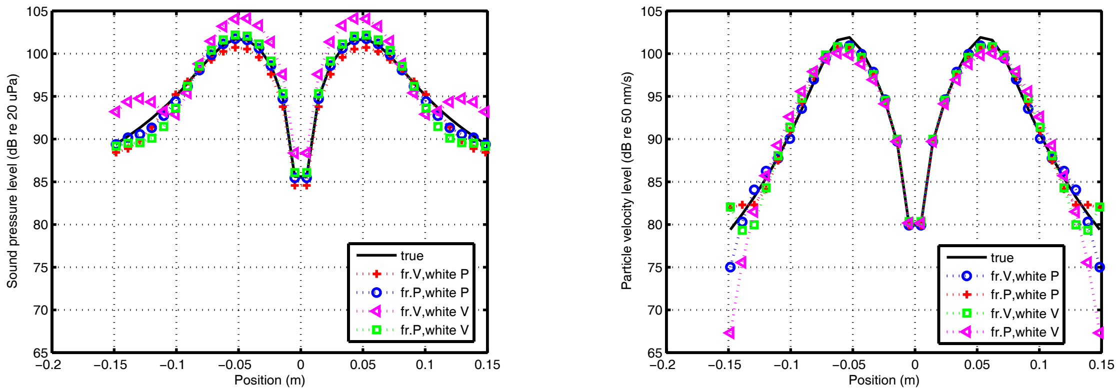

Figure 1. ‘True’ and reconstructed sound pressure (left) and particle velocity (right) in a diagonal across the prediction plane. Source: a dipole in the ‘source plane’.

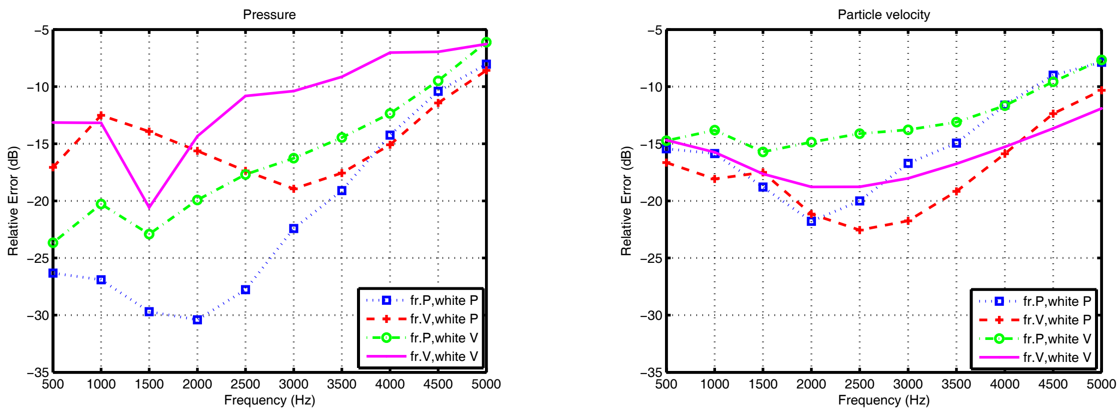

Figure 2. Relative global error of reconstructed sound pressure (left) and particle velocity (right) as a function of the frequency. Source: a dipole in the ‘source plane’.

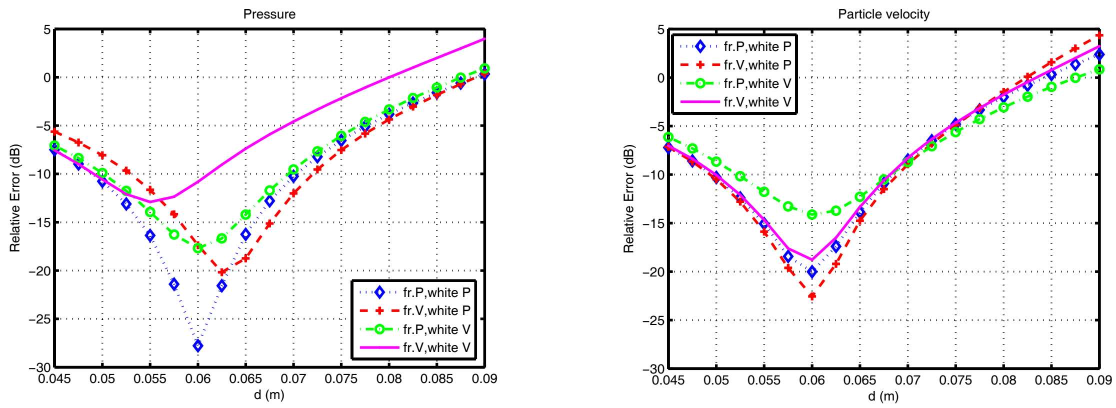

Figure 3. Relative global error of reconstructed sound pressure (left) and particle velocity (right) as a function of *d*. Source: a dipole, placed as above.

The first part of the study examines the four different sound pressure estimates and the four different particle velocity estimates separately. Figure 1 shows the 'true' and predicted sound pressure and particle velocity generated by a dipole at 2.5 kHz, placed in the 'source plane' at (0.04, 0.04, 0) [coordinates in m, and $z = 0$ is the 'source plane']. Note that the particle velocity is shown relative to 50 nm/s. The best prediction of the pressure is determined with eq. (1) ('fr. P, white P'); and prediction of the particle velocity determined with eq. (3) ('fr. V, white V') seems to be slightly better than the others. However, the pressure predictions are much more sensitive to the weighting of elementary waves than the particle velocity predictions, which are very similar.

The relative global error is shown in fig. 2 as a function of the frequency. It is apparent that a constant pressure wave weighting in general gives the best results, in particular when the pressure or particle velocity is predicted from the same quantity. Figure 3 shows the relative global error as a function of *d*; all other positions are the same as in the foregoing. It is clear that the best results are obtained with transfer matrices that correspond to the real source position. It can also be seen that a constant pressure wave weighting is favourable, and that the best results are obtained when the pressure is predicted from the pressure and the particle velocity is predicted from the particle velocity.

3.2 Infinite vibrating panels

The previous test cases indicated that a constant pressure wave weighting is in general the best option. It might be interesting to examine whether an extreme case can confirm that. Accordingly, the next simulation involves propagating bending waves on a conceptual *infinite* 5-mm steel plate. Such a vibrating infinite plate has a critical frequency of 2.44 kHz below which it generates evanescent waves and above which it generates propagating waves [1].

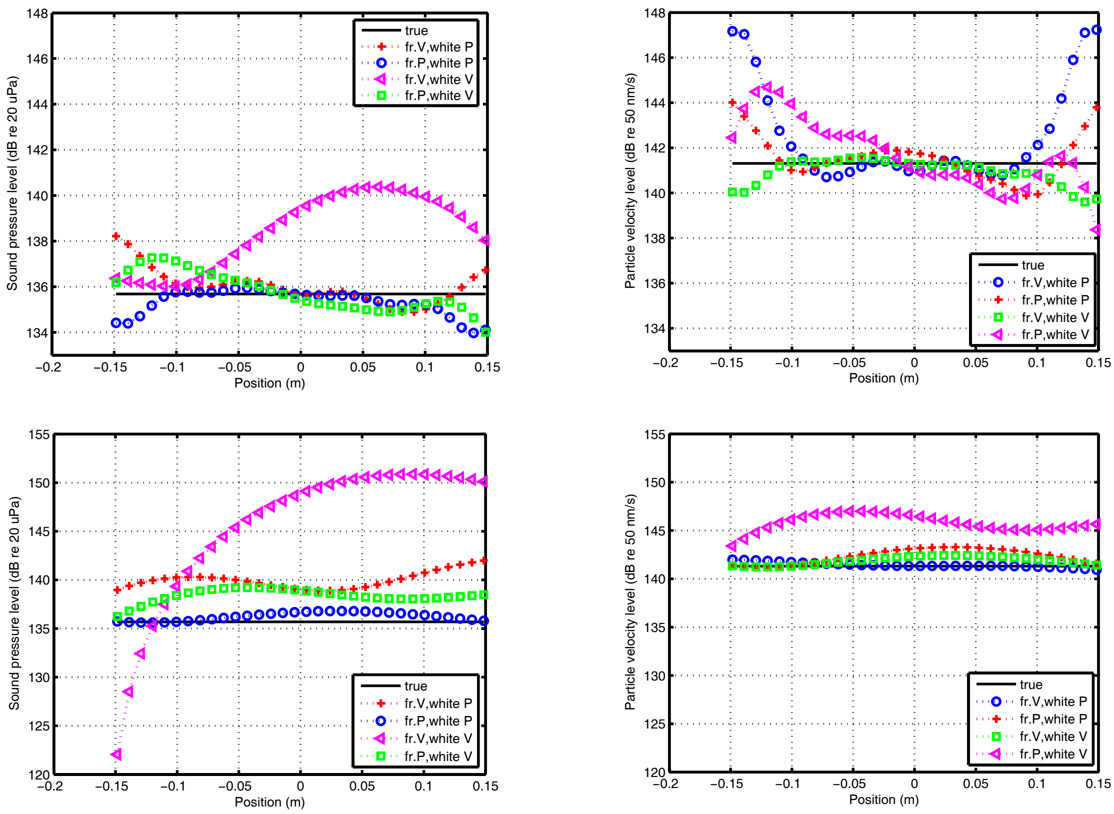

Figure 4. 'True' and reconstructed sound pressure (left column) and particle velocity (right column) in a diagonal across the prediction plane. Source: a subsonic bending wave on an infinite plate generating a purely evanescent sound field. Top row, d = 6 cm; bottom row, d = 12 cm.

Figure 4 shows the results of predicting the pressure and particle velocity at 500 Hz, where the plate generates a purely evanescent sound field. The predictions of the pressure confirm the advantage of a constant pressure wave weighting. However, the predictions of the particle velocity seem to be somewhat better when based on a constant velocity wave weighting. The bottom row shows the effect of increasing *d* from 6 to 12 cm (all other distances are unchanged). This obviously increases the prediction errors significantly, confirming that the transfer matrices should correspond to the real distance to the source. Figure 5 shows the results of predicting the plane propagating wave generated by the infinite plate when it vibrates at 3 kHz. The tendencies are the same as found in the top row of fig. 4.

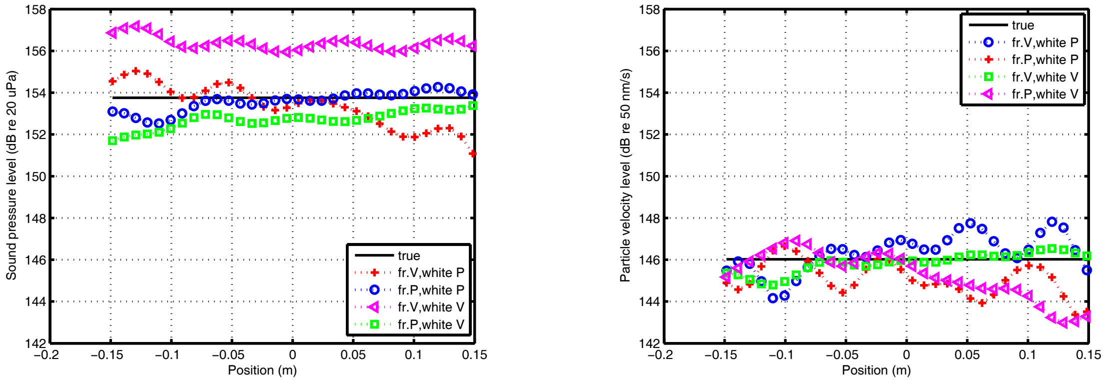

Figure 5. 'True' and reconstructed sound pressure (left) and particle velocity (right) in a diagonal across the prediction plane. Source: a supersonic bending wave on an infinite plate generating a propagating plane wave.

3.3 SONAH with a disturbing source

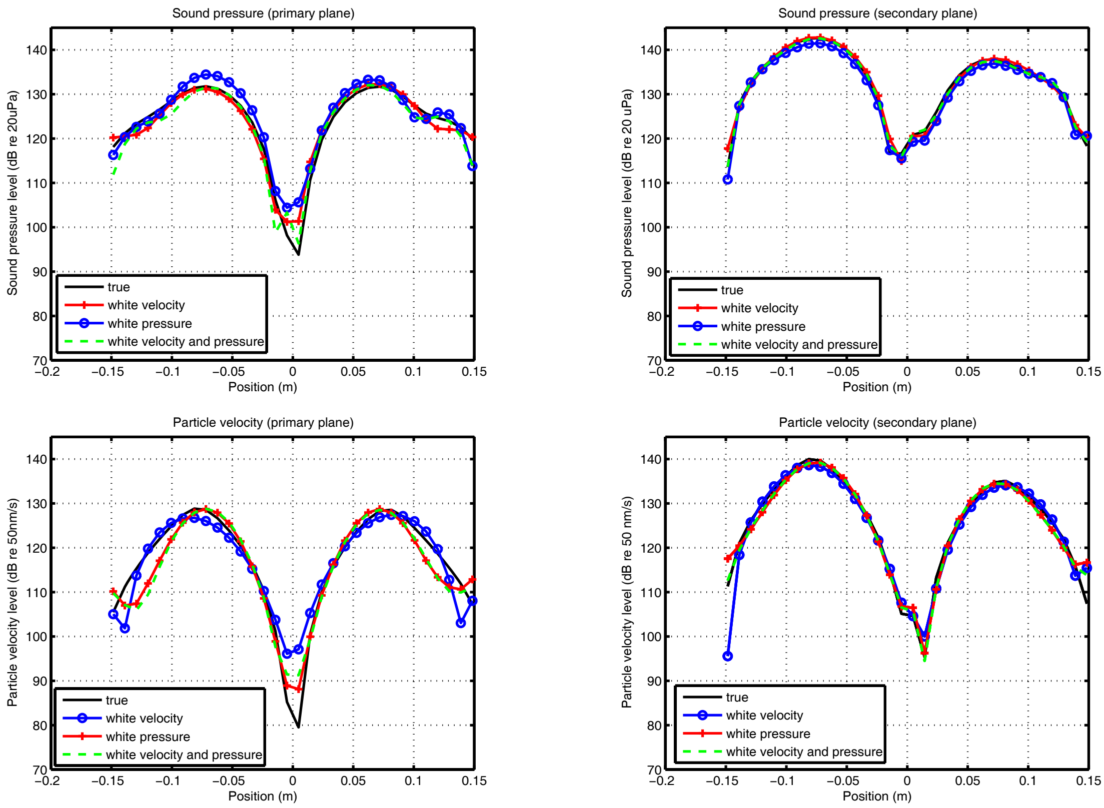

Figure 6. 'True' and reconstructed undisturbed sound pressure (top row) and particle velocity (bottom row) in a diagonal across the prediction plane. Left column, primary prediction plane; right column, secondary prediction plane. Sources: two parallel baffled vibrating panels.

The third part of the study is concerned with the '*p-u* method' described in section 2.4. Both the primary and the secondary source are simply supported steel panels with dimensions 1 x 1 m and a thickness of 5 mm, placed in infinite, rigid baffles and driven by point forces near a corner (but not at symmetrical positions, since that would generate a particle velocity of zero in the measurement plane). The panels are modelled as modal sums, and the radiated sound field is calculated using a numerical approximation to Rayleigh's first integral [1]. The panel on the 'wrong' side vibrates eight times stronger than the primary panel. Reflections from the baffled panels are ignored. (This is, of course, not realistic; the point is not realism but to test the *p-u* method's capability of suppressing sound from the 'wrong' side.) Figure 6 shows predictions of the undisturbed sound pressure and particle velocity in diagonals of the 'primary' and 'secondary' prediction plane when the plates are driven at 2.5 kHz, just above the critical frequency. As can be seen all the predictions are fairly accurate; and although the disturbing sound field is much stronger predictions of the undisturbed sound field generated by the primary source are acceptable. The weighting of elementary waves does not seem to have any significant systematic effect.

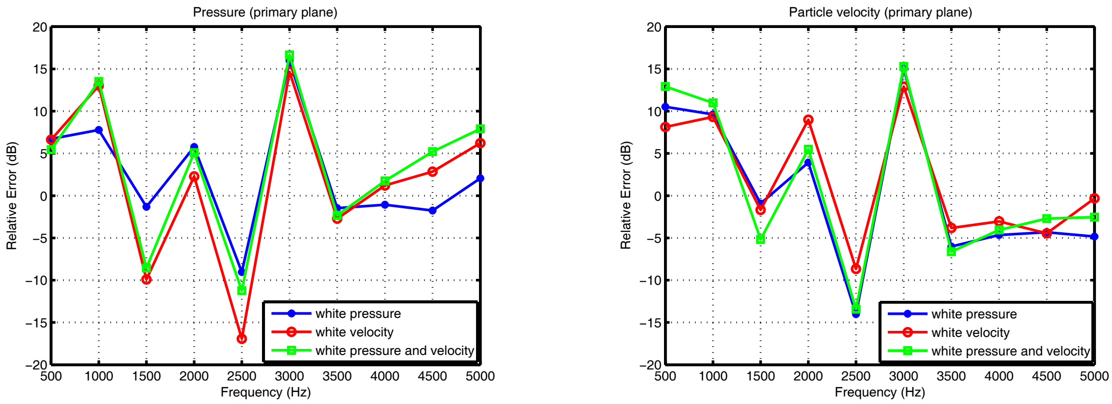

Figure 7. Relative global error of reconstructed undisturbed sound pressure (left) and particle velocity (right) in the primary prediction plane as a function of the frequency. Sources: two parallel baffled vibrating panels.

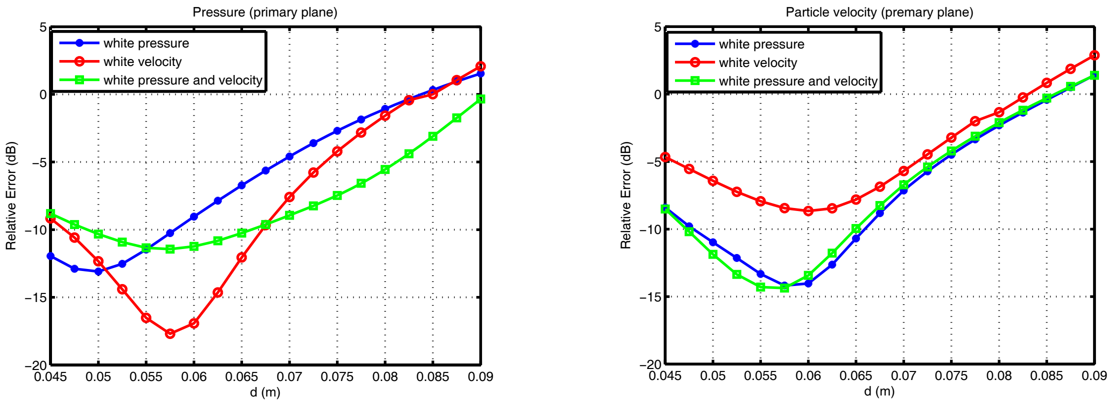

Figure 8. Relative global error of reconstructed undisturbed sound pressure (left) and particle velocity (right) in the primary prediction plane as a function of *d*. Sources: two parallel baffled vibrating panels.

Figure 7 shows the relative global error in the primary prediction plane as a function of the frequency. The error appears to vary erratically with the frequency, but there is no clear influence of the weighting of the elementary waves. Figure 8 shows the relative global error as a function of *d* (all other distances are unchanged). Again it is apparent that *d* should preferably be close to the physical distance between the source and the measurement plane. However, it seems that a constant pressure weighting of the elementary waves is less favourable for the *p-u* method that for predictions based only on the pressure or the particle velocity.

4. CONCLUSIONS

Statistically optimised near field acoustic holography (SONAH) is usually based on measurement of the sound pressure. In this work SONAH based on measurement of pressure and particle velocity has been examined with respect to the influence of the weighting of the elementary waves used in determining the SONAH transfer matrices and the influence of the position of the plane from which these elementary waves originate. In general pressure-based estimates of the pressure are better than particle velocity-based estimates, and particle velocity-based estimates of the particle velocity are better than pressure-based estimates. Different weightings of the elementary waves give slightly different results, and on the whole transfer matrices based on the elementary waves having a pressure amplitude of unity in the 'source plane' seem to perform somewhat better than transfer matrices based on elementary waves having a particle velocity amplitude of unity in the same plane.

The distance between the measurement plane and the plane at which the elementary waves originate has a significant influence on the results. The best predictions occur when this distance is close to the actual physical distance between the measurement plane and the source. A too large distance reduces the influence of the evanescent elementary waves and thus has a negative influence on the reproduction of evanescent near fields, but a too short distance is also unfavourable.

The *p-u* method based on combining pressure- and velocity-based estimates has also been examined. This method makes it possible to distinguish between sound coming from the two sides of the measurement plane, and the results demonstrate that it is indeed possible to reconstruct the undisturbed sound field generated by the primary source in the prediction plane even in the presence of much stronger noise from a source on the other side of the measurement plane. Somewhat surprisingly, the weighting of the elementary waves seems to have a different influence on the *p-u* method than on predictions based only on pressure or velocity, and the combination examined in ref. [6] seems to be a good compromise.

REFERENCES

[1] E.G. Williams, *Fourier Acoustics—Sound Radiation and Nearfield Acoustical Holography*, Academic Press, San Diego, 1999.

[2] R. Steiner and J. Hald, 'Near-field acoustical holography without the errors and limitations caused by the use of spatial DFT,' *Intern. J. Acoust. Vib.* **6**, 83-89 (2001).

[3] J. Hald, 'Patch near-field acoustical holography using a new statistically optimal method,' *Proc. Inter-Noise 2003*, Jeju Island, Korea, 2003, pp. 2203-2210.

[4] R. Raangs, W.F. Druyvesteyn and H.-E. de Bree, 'A low-cost intensity probe,' *J. Audio Eng. Soc.* **51**, 344-357 (2003).

[5] F. Jacobsen and Y. Liu, 'Near field acoustic holography with particle velocity transducers,' *J. Acoust. Soc. Am.* **118**, 3139-3144 (2005).

[6] F. Jacobsen and V. Jaud, 'Statistically optimized near field acoustic holography using an array of pressure-velocity probes,' *J. Acoust. Soc. Am.* **121**, 1550-1558 (2007).

[7] M. Tamura, 'Spatial Fourier transform method of measuring transmission coefficients at oblique incidence. I: Theory and numerical examples,' *J. Acoust. Soc. Am.* **88**, 2259-2264 (1990).

[8] J. Hald, 'Patch holography using a two-layer handheld array with an extended SONAH algorithm, *Proc. Euronoise*, Tampere, Finland, 2006.

[9] P.C. Hansen, *Rank-Deficient and Discrete Ill-Posed Problems: Numerical Aspects of Linear Inversion*, SIAM, Philadelphia, 1997.